Journal of Molecular and Cellular Cardiology 111 (2017) 51–60

Contents lists available at ScienceDirect

Journal of Molecular and Cellular Cardiology

journal homepage: www.elsevier.com/locate/yjmcc

The impact of ovariectomy on cardiac excitation-contraction coupling is mediated through cAMP/PKA-dependent mechanisms

Randi J. Parks [a], Oleg Bogachev [b], Martin Mackasey [b], Gibanananda Ray [b], Robert A. Rose [b], Susan E. Howlett [a,c,*]

[a] Department of Pharmacology, Faculty of Medicine, Dalhousie University, 5850 College Street, P.O. Box 15000, Halifax B3H 4R2, Nova Scotia, Canada
[b] Department of Physiology and Biophysics, Faculty of Medicine, Dalhousie University, 5850 College Street, P.O. Box 15000, Halifax B3H 4R2, Nova Scotia, Canada
[c] Department of Medicine (Geriatric Medicine), Faculty of Medicine, Dalhousie University, 5850 College Street, P.O. Box 15000, Halifax B3H 4R2, Nova Scotia, Canada

ARTICLE INFO

Article history:
Received 12 May 2017
Received in revised form 11 July 2017
Accepted 28 July 2017
Available online 01 August 2017

Keywords:
Estrogen
Sex difference
Excitation-contraction coupling
Phosphodiesterase
Adenylyl cyclase

ABSTRACT

Ovariectomy (OVX) promotes sarcoplasmic reticulum (SR) Ca^{2+} overload in ventricular myocytes. We hypothesized that the cyclic adenosine monophosphate (cAMP)/protein kinase A (PKA) pathway contributes to this Ca^{2+} dysregulation. Myocytes were isolated from adult female C57BL/6 mice following either OVX or sham surgery (surgery at ≈1 mos). Contractions, Ca^{2+} concentrations (fura-2) and ionic currents were measured simultaneously (37 °C, 2 Hz) in voltage-clamped myocytes. Intracellular cAMP levels were determined with an enzyme immunoassay; phosphodiesterase (PDE) and adenylyl cyclase (AC) isoform expression was examined with qPCR. Ca^{2+} currents were similar in myocytes from sham and OVX mice but Ca^{2+} transients, excitation-contraction (EC)-coupling gain, SR content and contractions were larger in OVX than sham cells. To determine if the cAMP/PKA pathway mediated OVX-induced alterations in EC-coupling, cardiomyocytes were incubated with the PKA inhibitor H-89 (2 μM), which abolished baseline differences. While basal intracellular cAMP did not differ, levels were higher in OVX than sham in the presence of a non-selective PDE inhibitor (300 μM IBMX), or an AC activator (10 μM forskolin). This suggests the production of cAMP by AC and its breakdown by PDE were enhanced by OVX. Consistent with this, mRNA levels for both AC5 and PDE4A were higher in OVX in comparison to sham. Differences in Ca^{2+} homeostasis and contractions were abolished when sham and OVX cells were dialyzed with patch pipettes containing the same concentration of 8-bromoadenosine-cAMP (50 μM). Interestingly, selective inhibition of PDE4 increased Ca^{2+} current only in OVX cells. Together, these findings suggest that estrogen suppresses SR Ca^{2+} release and that this is regulated, at least in part, by the cAMP/PKA pathway. These changes in the cAMP/PKA pathway may promote Ca^{2+} dysregulation and cardiovascular disease when ovarian estrogen levels fall. These results advance our understanding of female-specific cardiomyocyte mechanisms that may affect responses to therapeutic interventions in older women.

1. Introduction

The risk of cardiovascular disease is lower in pre-menopausal women in comparison to age-matched men, but this advantage disappears as early as five years post-menopause [6,14,16]. Menopause is characterised by a decrease in the production of ovarian hormones, so it has been hypothesized that female sex steroid hormones regulate cardiac physiology and pathophysiology [28,49]. Over 50 observational studies have found that hormone replacement therapy in post-menopausal women causes a reduction in cardiovascular events [17]. However, cardioprotective effects of estrogen remain controversial, as two randomized controlled clinical trials have reported no cardiovascular benefits [20,31,33]. A recent prospective trial reported an improvement in several blood markers for cardiovascular disease in women receiving hormone replacement therapy within three years of menopause, although the long-term effects remain unclear [15,27]. These inconclusive results highlight the importance of understanding how female sex steroid hormones affect cardiovascular function.

Cardiomyocytes possess receptors for all three major sex steroid hormones (estrogen, progesterone and testosterone), therefore sex hormones may affect myocardial function by acting on individual myocytes [11,29]. A number of studies have examined isolated ventricular myocytes from sham-operated and ovariectomized (OVX) mice to investigate the effects of ovarian hormone withdrawal on Ca^{2+} homeostasis and excitation-contraction (EC) coupling. OVX causes a marked

Abbreviations: OVX, ovariectomized; EC-coupling, excitation-contraction coupling; SR, sarcoplasmic reticulum; cAMP, cyclic AMP; PKA, protein kinase A; PDE, phosphodiesterase; AC, adenylyl cyclase.

* Corresponding author at: Department of Pharmacology, Dalhousie University, 1459 Oxford Street, Sir Charles Tupper Medical Building, PO Box 15000, Halifax B3H 4R2, Nova Scotia, Canada.
E-mail addresses: Randi.Parks@nih.gov (R.J. Parks), ol798526@dal.ca (O. Bogachev), MMackasey@dal.ca (M. Mackasey), Giban.Ray@dal.ca (G. Ray), Robert.Rose@dal.ca (R.A. Rose), Susan.Howlett@dal.ca (S.E. Howlett).

http://dx.doi.org/10.1016/j.yjmcc.2017.07.118
0022-2828/

increase in sarcoplasmic reticulum (SR) Ca^{2+} content, augments SR Ca^{2+} release and promotes Ca^{2+} overload in ventricular myocytes [10,12,25,30]. Overall, these findings suggest that estrogen modifies Ca^{2+} handling in individual myocytes. As myocardial Ca^{2+} overload is involved in the pathogenesis of many cardiovascular diseases [5], it is important to investigate the mechanisms underlying how ovarian hormones may alter Ca^{2+} handling in cardiomyocytes.

Myocardial Ca^{2+} homeostasis is regulated by the cyclic AMP (cAMP)/protein kinase A (PKA) pathway, even in the absence of β-adrenergic stimulation [5,35]. In addition, there are important male-female differences in the cAMP/PKA pathway. Our group has previously shown that intracellular cAMP levels are lower in ventricular myocytes from females when compared to males, which is due to higher phosphodiesterase (PDE) 4B expression in females [36]. Further, inhibition of PKA was found to abolish male-female differences in SR Ca^{2+} release and contractions seen in cardiomyocytes. Thus, estrogen may alter SR Ca^{2+} release by modifying one or more components of the cAMP/PKA pathway, such as cAMP production by adenylyl cyclase (AC) or degradation by PDE, to affect downstream phosphorylation of key components of EC-coupling. There are various isoforms of both AC and PDE in the heart, primarily AC5 and AC6, and PDE3 and PDE4 [8,18]. Further, cAMP signaling within cardiomyocytes has been shown to be compartmentalized by different PDE isoforms [1,2], but only male models have been examined so whether sex steroid hormones affect cAMP signaling has not been explored. Although information is limited, OVX has been shown to increase PKA expression and activity in myocytes from OVX rats [23,25]. Whether OVX affects other components of the cAMP/PKA pathway, such as cAMP production or degradation, and how this may impact EC-coupling and Ca^{2+}-induced Ca^{2+} release from the SR, has not been investigated.

The objectives of this study were: 1) to determine whether OVX affects cAMP/PKA-mediated cellular mechanisms that regulate SR Ca^{2+} release and EC-coupling, and 2) to determine how OVX modifies the cAMP/PKA pathway, including effects on cAMP production by AC and breakdown by PDE. In these studies, contractions, Ca^{2+} transients and Ca^{2+} currents were simultaneously recorded in ventricular myocytes from sham and OVX female mice. The cAMP/PKA pathway was pharmacologically activated or inhibited to identify the EC-coupling mechanisms involved. Cyclic AMP was measured with an enzyme immunoassay, while qPCR was used to assess AC and PDE expression. Results indicate that OVX increases both the production and breakdown of cAMP, which suggests that ovarian hormones may attenuate cAMP/PKA-dependent mechanisms involved in cardiac EC-coupling.

2. Materials and methods

2.1. Animals and body composition

Experiments conformed to the Canadian Council on Animal Care Guide to the Care and Use of Experimental Animals (CCAC, Ottawa, ON: Vol. 1, 2nd ed., 1993; Vol. 2, 1984) and were approved by the Dalhousie University Committee on Laboratory Animals. Animals were purchased from Charles River Laboratories (St. Constant, QC). OVX mice were subjected to a bilateral removal of the ovaries through a dorsal midline skin incision at approximately 1 month of age and sham-operated controls were subjected to a similar surgery, but the ovaries were left intact as in our previous study [12]. Mice were aged to approximately 8 months of age prior to experiments; OVX was confirmed by uterine atrophy. This time frame was selected to examine effects of long-term ovarian hormone withdrawal and to allow comparisons with our earlier work [12].

2.2. Isolation of ventricular myocytes

Ventricular myocytes were isolated as previously described [36]. In brief, hearts were cannulated in situ through the aorta, excised, and perfused retrogradely at 2.2 ml/min for 10 min with nominally Ca^{2+}-free solution (mM): 105 NaCl, 5 KCl, 25 HEPES, 0.33 NaH_2PO_4, 1 $MgCl_2$, 20 glucose, 3 Na-pyruvate, 1 lactic acid (100% O_2; pH 7.4; 37 °C). The heart was then perfused with the same solution plus 50 μM Ca^{2+}, collagenase (8 mg/30 ml, Worthington Type I, 250 U/mg), dispase II (3.5 mg/30 ml, Roche) and trypsin (0.5 mg/30 ml) for 8–9 min. The ventricles were minced in high K^+ buffer (mM): 50 L-glutamic acid, 30 KCl, 30 KH_2PO_4, 20 taurine, 10 HEPES, 10 glucose, 3 $MgSO_4$ and 0.5 EGTA (pH 7.4; room temp). Tissue was gently agitated and the supernatant was filtered with a 225 μm polyethylene filter (Spectra/Mesh).

2.3. Electrophysiology

Myocytes were placed in a custom-made glass-bottomed chamber mounted on the stage of an inverted microscope (Nikon Eclipse, TE200, Nikon Canada, Mississauga, ON) and incubated with the Ca^{2+}-sensitive fluorescent dye fura-2 acetoxymethyl (AM) ester (5 μM; Invitrogen, Burlington, ON) for 20 min in the dark in the high K^+ buffer described in Section 2.2. Cells were superfused at 3 ml/min with HEPES buffer (mM): 145 NaCl, 10 glucose, 10 HEPES, 4 KCl, 1 $CaCl_2$, 1 $MgCl_2$, 4,4-aminopyridine to inhibit transient outward K^+ current, and 0.3 lidocaine to inhibit Na^+ current (pH 7.4; 37 °C). Na^+ current was also inactivated by giving the cell a pre-pulse to −40 mV prior to test pulses. Quiescent rod-shaped myocytes with clear striations were selected for experiments. For high-resistance voltage-clamp experiments, membrane potentials and currents were recorded by impaling cells with microelectrodes (18–30 MΩ) filled with filtered 2.7 M KCl. In patch-clamp experiments, myocytes were voltage-clamped with fire-polished patch pipettes (1–3 MΩ) filled with (mM): 70 KCl, 70 potassium aspartate, 4 Mg-ATP, 1 $MgCl_2$, 2.5 KH_2PO_4, 0.12 $CaCl_2$, 0.5 EGTA, and 10 HEPES (pH 7.2). In some cases, the patch pipette solution also contained 50 μM 8-Bromo-cAMP (8-Br-cAMP). An Axoclamp 2B amplifier (Molecular Devices, Sunnyvale, CA; 5–6 Hz) was used for discontinuous single electrode voltage-clamp and ClampEx v8.2 software (Molecular Devices) was used to generate protocols. Five 50 ms conditioning pulses from −80 to 0 mV (2 Hz) were delivered to cells, followed by repolarization to −40 mV for 450 ms. As previously described, Ca^{2+} currents, Ca^{2+} transients and contractions were recorded simultaneously during 250 ms test pulses from −40 to 0 mV [36]. Ca^{2+} current was measured as the difference between peak current and the end of the test pulse and was normalized to cell capacitance, which was determined by integrating capacitive transients. Fractional shortening (%) was calculated by normalizing contraction (diastolic cell length – peak contraction) to diastolic length.

Fura-2 was alternately excited with 340 and 380 nm light and fluorescence emission was measured at 510 nm (5 ms sampling interval) with a DeltaRam fluorescence system and Felix v1.4 software (PTI) to measure intracellular Ca^{2+} concentrations. Background fluorescence recordings made at each wavelength were subtracted from their respective experimental recordings. The resulting background-subtracted ratio of emissions was used to convert ratios to intracellular Ca^{2+} concentrations with an in vitro calibration curve, as previously described [44]. Briefly, the calibration curve was generated using methods adapted from Grynkiewicz et al. [13] where serial additions of a Ca^{2+}-containing, EGTA-buffered solution were made to a Ca^{2+}-free EGTA-buffered solution to generate a range of different Ca^{2+} concentrations. Fluorescence ratios for the different Ca^{2+} concentrations were recorded and a calibration curve was generated. Fluorescence data were analyzed with Felix (PTI) and Clampfit software. Diastolic Ca^{2+} was measured at −80 mV, and Ca^{2+} transient amplitudes were determined as the difference between peak systolic Ca^{2+} and the Ca^{2+} concentration prior to the test pulse, at −40 mV. The gain of EC-coupling was calculated as the absolute value of the Ca^{2+} transient (nM) per unit of normalized Ca^{2+} current (pA/pF). Responses were not averaged or filtered prior to analysis.

As previously described, SR Ca^{2+} content was measured in voltage-clamped cells. Following a series of conditioning pulses, cells were held at −60 mV and 10 mM caffeine was rapidly applied for 1 s. The caffeine solution contained (mM): 10 caffeine, 140 LiCl, 4 KCl, 10 glucose, 5 HEPES, 4 $MgCl_2$, 4,4-aminopyridine, and 0.3 lidocaine. Caffeine solution was nominally Ca^{2+}- and Na^{+}-free to inhibit extrusion of Ca^{2+} from the cytosol by Na^{+}-Ca^{2+} exchange. SR Ca^{2+} stores were measured as the peak caffeine-induced Ca^{2+} transient. Fractional release, which represents the amount of Ca^{2+} released on each beat as a fraction of the amount available for release in the SR, was calculated by dividing Ca^{2+} transient by caffeine transient amplitude and expressing this value as a percent. Responses were not averaged or filtered prior to analysis.

For experiments with the PKA inhibitor H-89 (2 μM), a minimum 30 min drug exposure preceded recordings, as previously reported [51]. For forskolin (10 μM), rolipram (10 μM) and IBMX (300 μM), recordings were made following a minimum 10 min drug exposure [19,35]. No further effects were seen with longer incubation times. DMSO solvent controls (0.02 to 0.06%) had no effect on Ca^{2+} currents, Ca^{2+} transients or contractions. All drug treatments were performed on different cells than those used for recording basal responses.

2.4. cAMP enzyme immunoassay

Intracellular cAMP levels were determined as previously reported [36]. Briefly, aliquots of isolated myocytes were centrifuged (~70 min, 18 g), resuspended in HEPES buffer, and incubated for 1 h at room temperature in 96-well plates (~1000 cells/well). Cells were treated with DMSO solvent control (0.1%), forskolin (1 or 10 μM), or IBMX (300 μM) for 10 min prior to cell membrane rupture (0.25% dodecyltrimethylammonium bromide; 10 min). Cell lysates were stored at −20 °C. Intracellular cAMP levels were determined in acetylated cell lysates using an Amersham™ cAMP Biotrak™ Enzyme immunoassay System (GE Healthcare Life Sciences, Baie d'Urfe, QC). A plate reader (450 nm, ELx800, BioTek Instruments, Winooski, VT) measured sample absorbances, which were compared to a cAMP standard curve (2 to 128 fmol cAMP; $r^2 = 0.99$). cAMP concentrations were normalized to the amount of protein in each sample, determined with a detergent-compatible Lowry assay kit (BioRad, Mississauga, ON).

2.5. Quantitative PCR

The heart was excised from the mouse and the apex was used for analysis by quantitative PCR. The tissue was snap frozen in liquid nitrogen and stored at −80 °C until being further processed for quantitative gene expression analysis. Primers were designed for mouse AC isoforms 4, 5, 6, and 9, PDE isoforms 3A, 3B, 4A, 4B, and 4D and GAPDH, which was used as a reference gene (Refer to Supplemental Table 1 for all primer sequences). Primers were synthesized (Sigma-Aldrich and Invitrogen) and reconstituted in nuclease free water at a concentration of 100 nM and stored at −20 °C. All primer sets underwent validation tests to determine optimal annealing temperatures as well as confirmation of an ideal amplification efficiency (between 90 and 110% copy efficiency per cycle)

RNA was extracted in PureZOL™ RNA isolation reagent according to kit instructions (Aurum Total RNA Fatty and Fibrous Tissue Kit, Bio-Rad). Tissue was eluted in 40 μl of elution buffer from the spin column. RNA concentrations were determined using a Qubit fluorometer (Invitrogen) and first strand synthesis reactions were performed using the iScript cDNA synthesis kit (BioRad) per kit instructions. The Experion™ Automated Electrophoresis System (Bio-Rad) was used to assess RNA quality by observing the 28S and 18S rRNA subunits prior to first strand synthesis. Sample purity was assessed using the Nanodrop lite system (Thermo Scientific). Lack of genomic DNA contamination was verified by reverse transcription (RT)-PCR using a no RT control.

RT-qPCR using BRYT green dye (Promega) was used to assess gene expression. Following RNA extraction, cDNA was synthesized and 10 μl reactions were performed with 5.6 μl of BRYT green dye, 4 μl cDNA template (at the appropriate dilution), and 0.4 μl of primers. Primers were used at a concentration of 10 nM. Reactions were carried out using the CFX384 Touch™ Real-Time PCR Detection System (Bio-Rad). Amplification conditions were as follows: 95 °C for 2 min to activate Taq polymerase, followed by 39 cycles of denaturation at 95 °C for 15 s, annealing at 60 °C for AC, or 53–61 °C for PDE for 30 s, and extension at 72 °C for 30 s. Melt curve analysis was performed from 65 to 95 °C in 0.5 °C increments. Single amplicons with appropriate melting temperatures and sizes were detected. Data were analyzed using the $2^{-\Delta\Delta C}{}_T$ method by which the expression values are relative to an internal control and normalized to GAPDH. mRNA levels for all tissue samples were expressed in the form of $2^{-CT} \times 100$ versus GAPDH.

2.6. Statistical analyses

Sigmaplot (v11.0, Systat Software Inc.) was used for all statistical analyses. Differences between means ± S.E.M. were tested with Students *t*-test or two-way analysis of variance (ANOVA). All drug treatment data were analyzed with two-way ANOVA, using animal OVX status and drug condition as the two independent factors. Post hoc pairwise comparisons were done using the Holm-Sidak method. All figures were constructed with Sigmaplot.

2.7. Chemicals

All chemicals, unless otherwise stated, were purchased from Sigma-Aldrich (Oakville, ON) or BDH Inc. (Toronto, ON). Fura-2 AM was prepared in anhydrous DMSO and stored at −20 °C. H-89 and rolipram were dissolved in DMSO and stored at −20 °C. Forskolin was dissolved in DMSO and stored at room temperature. IBMX was dissolved in DMSO with mild heating and stored at −20 °C.

Table 1
Physical and cellular characteristics of sham and OVX female C57BL/6 mice.

Parameter	Sham	OVX	*P*-value
Age (mos)[a]	8.5 ± 0.2	8.6 ± 0.2	$P = 0.72$
Dry uterine weight (mg)[a]	17 ± 0.5	2.9 ± 0.2	$P < 0.001$*
Body weight (g)[a]	32.7 ± 1.0	37.1 ± 1.0	$P = 0.004$*
Heart weight (mg)	264 ± 7	267 ± 9	$P = 0.83$
Heart to body weight (mg/g)	8.3 ± 0.5	7.5 ± 0.3	$P = 0.20$
Heart weight to tibia length (mg/mm)	14.4 ± 0.4	14.1 ± 0.5	$P = 0.69$
Cell length (μm)	125 ± 2	122 ± 3	$P = 0.40$
Cell width (μm)[b]	31 ± 2	28 ± 1	$P = 0.18$
Cell area (μm^2)[b]	3810 ± 257	3600 ± 168	$P = 0.49$
Capacitance (pF)	227 ± 8	217 ± 5	$P = 0.31$

$n = 9$ sham and 9 OVX hearts; 43 sham and 52 OVX cells, unless indicated otherwise.
[a] $n = 36$ sham and 33 OVX mice.
[b] $n = 15$ sham and 17 OVX cells.
* Denotes significant for $P < 0.05$.

3. Results

3.1. OVX does not alter heart weight or myocyte size in female C57BL/6 mice

Physical characteristics of the sham and OVX animals are summarized in Table 1, as well as characteristics of the hearts and ventricular myocytes from these mice. Uterine dry weights were significantly lower in OVX mice than sham mice of the same age, indicative of uterine atrophy. OVX mice were heavier than sham controls. Mean heart weights did not differ between the two groups, even when heart weight was normalized to either body weight or tibia length. Ventricular myocytes from the two groups were similar in length, width and cross-sectional area; cell capacitance, a measure of total membrane

area, was also similar in the two groups (Table 1). These observations suggest that OVX does not cause cardiac hypertrophy in female mice.

3.2. OVX myocytes have larger contractions, Ca^{2+} transients and higher EC coupling gain

To determine how ovarian hormones affect basal cardiac contractile function, ventricular myocytes from sham and OVX mice were voltage-clamped and contractions, Ca^{2+} transients, and Ca^{2+} currents were simultaneously measured during a test step to 0 mV. Fig. 1A shows representative contractions, Ca^{2+} transients and Ca^{2+} currents in sham and OVX myocytes. Mean data show that contractions, expressed as fractional shortening, were larger in OVX myocytes in comparison to sham (Fig. 1B). Underlying Ca^{2+} transients were also larger in OVX than in sham cells (Fig. 1C). To determine if differences in Ca^{2+} transients were due to differences in Ca^{2+}-induced Ca^{2+} release from the SR, Ca^{2+} current was also compared and was similar in myocytes from sham and OVX mice (Fig. 1D). The amplification of Ca^{2+}-induced Ca^{2+} release from the SR, called the gain of EC-coupling, was then quantified as the ratio of Ca^{2+} transient to peak Ca^{2+} current. Gain was higher in OVX than in sham cells (Fig. 1E). By contrast, diastolic Ca^{2+} concentrations were not affected by OVX (Fig. 1F). These results demonstrate that myocytes from OVX mice have larger contractions and Ca^{2+} transients, as well as increased EC-coupling gain when compared to sham controls.

As PKA activity may increase following OVX [23], this could increase PKA-dependent phosphorylation of EC coupling components and augment SR Ca^{2+} release. To determine whether the changes in EC coupling mechanisms in OVX were attenuated by PKA inhibition, voltage-clamp experiments were performed in the absence and presence of the PKA inhibitor H-89 (2 μM). Fig. 2A shows example recordings of contractions, Ca^{2+} transients and Ca^{2+} currents from sham and OVX myocytes in the presence of 2 μM H-89. Inhibition of PKA with H-89 did not affect contractions in sham cells, but reduced fractional shortening in OVX cells and removed the difference between sham and OVX, as demonstrated by the dotted lines indicating basal values (Fig. 2B). H-89 also reduced Ca^{2+} transients in both sham and OVX myocytes and removed the difference present under basal conditions (Fig. 2C). This effect of PKA inhibition on Ca^{2+} transients was not due to changes in Ca^{2+} current, as peak Ca^{2+} current was not affected by H-89 in either group (Fig. 2D). Importantly, the basal difference in EC coupling gain was eliminated by PKA inhibition, as H-89 reduced gain in OVX, but not in sham cells (Fig. 2E). Diastolic Ca^{2+} was not affected by H-89 and remained similar

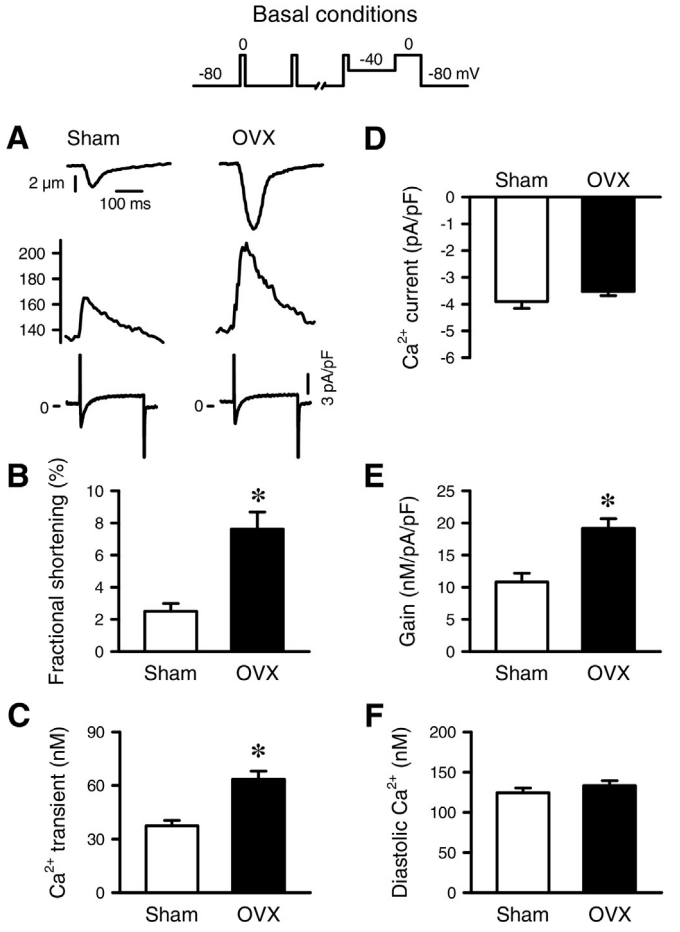

Fig. 1. Contractions, Ca^{2+} transients and the gain of EC coupling are larger in myocytes from OVX than sham female mice. The voltage clamp protocol used is shown in the top panel. A. Examples of contractions (top), Ca^{2+} transients (middle) and Ca^{2+} currents (bottom) from myocytes from a sham and OVX mouse. B. Mean fractional shortening was larger in OVX myocytes than sham. C. Ca^{2+} transients were also larger in OVX in comparison to sham. D. OVX and sham myocytes had similar Ca^{2+} currents. E. As such, the gain of EC coupling was higher in OVX than in sham cells. F. Diastolic Ca^{2+} did not differ between sham and OVX. (For contractions, $n = 15$ sham, 18 OVX cells. For other parameters, $n = 27$ sham, 38 OVX cells; 13 sham and 18 OVX mice. * denotes $P < 0.05$, by t-test).

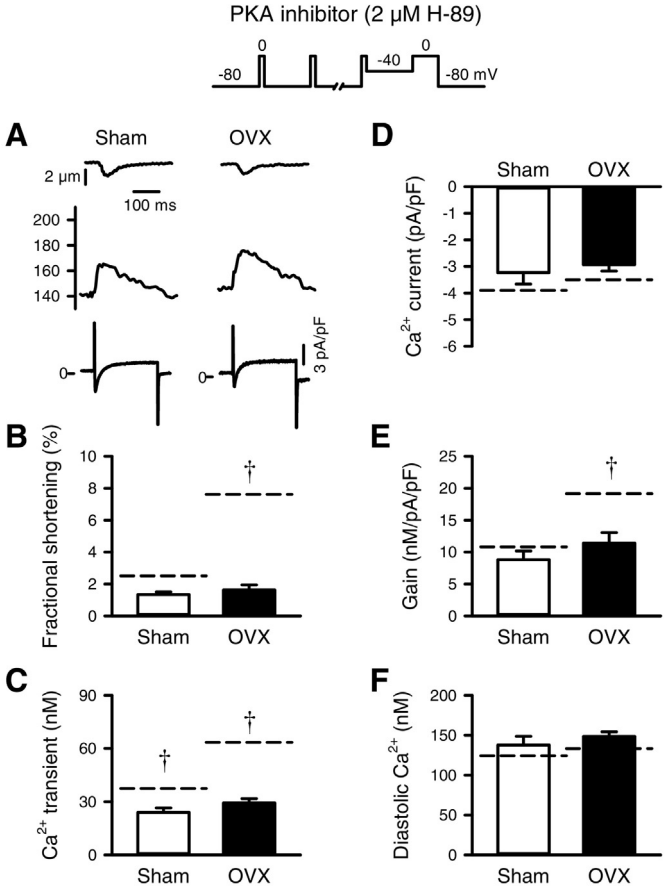

Fig. 2. Inhibition of PKA abolishes differences in contraction, Ca^{2+} transients and gain between sham and OVX myocytes. The top panel shows the voltage clamp protocol. A. Representative contractions (top), Ca^{2+} transients (middle) and Ca^{2+} currents (bottom) from sham and OVX myocytes in the presence of 2 μM H-89. B. H-89 decreased fractional shortening in OVX myocytes and abolished the basal difference. C. Ca^{2+} transients were smaller in both sham and OVX cells in the presence of H-89, and the basal difference was no longer present. D. H-89 did not affect Ca^{2+} current in sham or OVX mice. E. EC coupling gain was decreased by H-89 in OVX myocytes only, and the basal difference between sham and OVX was removed. F. Diastolic Ca^{2+} was unaffected by PKA inhibition. (For contractions, $n = 3$ sham, 5 OVX cells. For other parameters, $n = 10$ sham, 19 OVX cells; 5 sham, 7 OVX mice. * denotes $P < 0.05$ versus sham by 2-way ANOVA; † denotes $P < 0.05$ in comparison to same-group basal; dotted lines represent basal values).

in sham and OVX cells (Fig. 2F). These results demonstrate that inhibition of PKA abolished the increase in contractions, Ca^{2+} transients and EC-coupling gain characteristic of OVX myocytes.

These findings suggest that the cAMP/PKA pathway is involved in the increase in SR Ca^{2+} release observed following withdrawal of ovarian hormones. We hypothesized that exposing sham and OVX myocytes to the same concentration of intracellular cAMP would abolish differences in EC-coupling between the two groups. This was investigated by patch-clamping cells with pipettes filled with the cell-permeant, PDE-resistant cAMP analog 8-Br-cAMP. Fig. 3A depicts contractions, Ca^{2+} transients and Ca^{2+} currents recorded from myocytes dialyzed with 50 μM 8-Br-cAMP. Dialysis with 8-Br-cAMP increased fractional shortening in sham myocytes, but had no effect on fractional shortening in cells from OVX animals (Fig. 3B). Thus, the difference present under basal conditions (dotted lines) was abolished. Similarly, dialysis with 8-Br-cAMP increased peak Ca^{2+} transients only in sham cells (Fig. 3C) and eliminated the difference observed under basal conditions (dotted lines). Dialysis of cells with 8-Br-cAMP increased Ca^{2+} current to a similar extent in both sham and OVX myocytes (Fig. 3D). As a result, 8-Br-cAMP reduced gain in sham and OVX cells and eliminated the basal difference in gain between the two groups (Fig. 3E). Diastolic Ca^{2+} levels declined equally in both groups in the presence of 8-Br-cAMP (Fig. 3F). These results indicate that exposing sham and OVX myocytes to the same concentration of intracellular cAMP eliminates differences in contractions, Ca^{2+} transients, and EC-coupling gain seen under basal conditions.

3.3. OVX myocytes have higher SR Ca^{2+} stores, but this difference is abolished by H-89 or 8-Br-cAMP

Differences in Ca^{2+} transients and EC-coupling gain between sham and OVX myocytes could be due to changes in SR Ca^{2+} stores following ovarian hormone withdrawal. This was examined by measuring caffeine transients in voltage-clamped myocytes. Fig. 4A shows representative caffeine transients recorded in sham and OVX cells under basal conditions. SR Ca^{2+} stores were higher in OVX cells in comparison to sham controls (Fig. 4B). On the other hand, fractional release of SR Ca^{2+} (ratio of Ca^{2+} transient to caffeine transient) did not differ

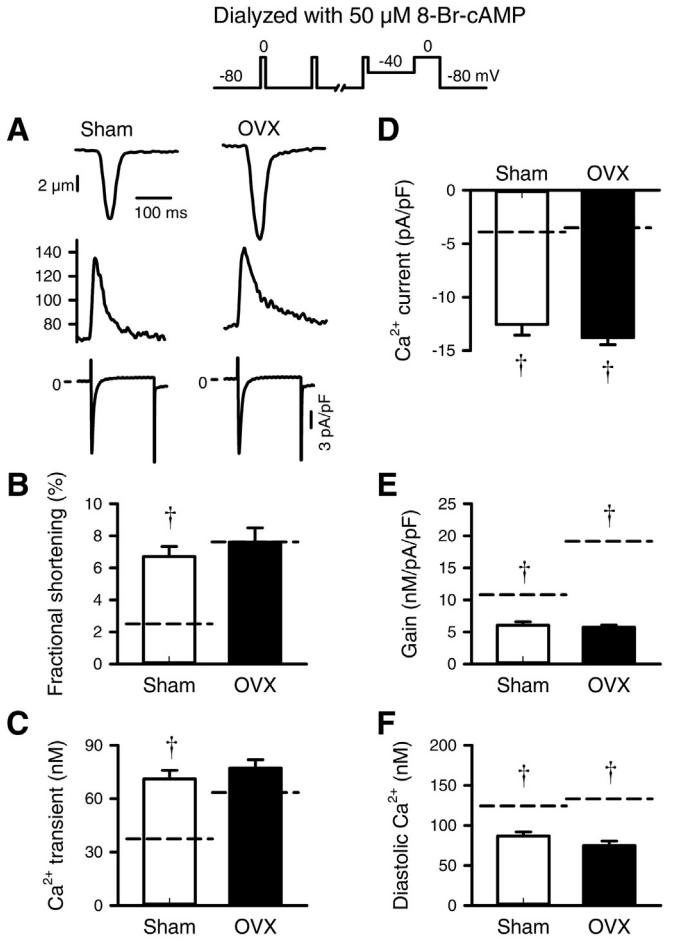

Fig. 3. Exposing myocytes from sham and OVX female mice to the same intracellular cAMP removes differences in contraction, Ca^{2+} transient and gain. The voltage clamp protocol used for patch clamp experiments is shown in the top panel. A. Examples of contractions (top), Ca^{2+} transients (middle) and Ca^{2+} currents (bottom) recorded in sham and OVX myocytes dialyzed with 50 μM 8-Br-cAMP. B. Fractional shortening was increased in sham upon dialysis with cAMP, and the basal difference was abolished. C. Dialysis of sham and OVX cells with cAMP increased Ca^{2+} transients in sham cells only and abolished the basal difference. D. Ca^{2+} current was increased in sham and OVX cells and remained similar between the two groups. E. Dialysis with 8-Br-cAMP decreased gain in myocytes from sham and OVX mice, and the difference present under basal conditions was removed. F. 8-Br-cAMP decreased diastolic Ca^{2+} levels in both sham and OVX. (For contractions, $n = 11$ sham, 14 OVX cells. For other parameters, $n = 14$ sham, 15 OVX cells; 8 sham, 8 OVX mice. * denotes $P < 0.05$ versus sham by 2-way ANOVA; † denotes $P < 0.05$ versus same-group basal; dotted lines represent basal values).

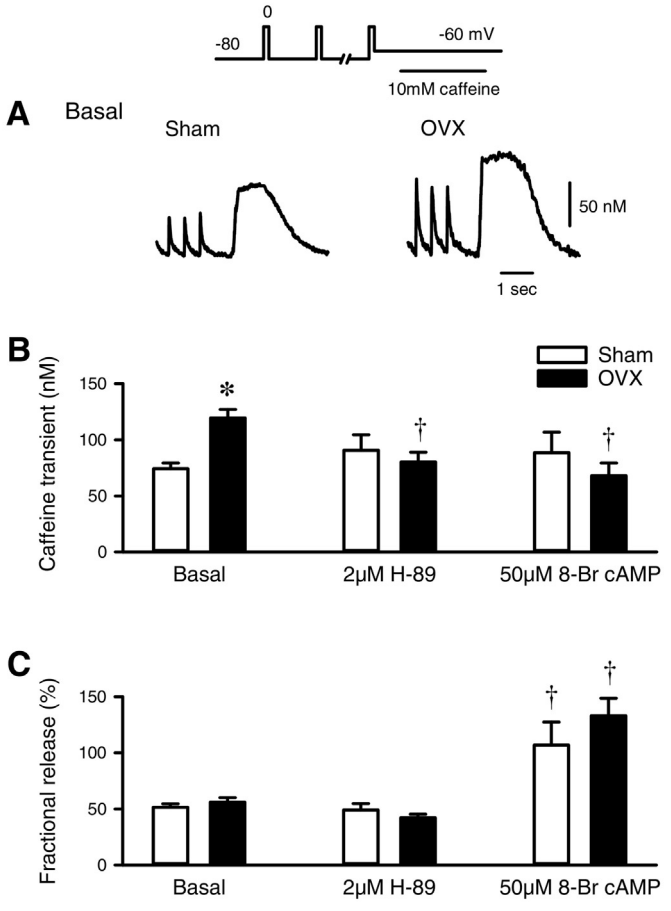

Fig. 4. SR Ca^{2+} stores are increased in OVX myocytes in comparison to sham, and either inhibition of PKA or dialysis with 8-Br-cAMP abolished this difference. The voltage clamp protocol used in shown in the top panel, and indicates the rapid application of 10 mM caffeine (1 s). A. Example caffeine transients recorded from a sham and an OVX myocyte. B. SR Ca^{2+} stores, determined by caffeine transients, were higher in cells from OVX mice in comparison to sham under basal conditions. Inhibition of PKA with H-89 (2 μM) reduced SR Ca^{2+} stores in OVX myocytes only, and abolished the basal difference. Similarly, dialysis of myocytes with 8-Br-cAMP (50 μM) decreased caffeine transients in OVX cells and removed the difference present under basal conditions. C. Fractional SR Ca^{2+} release was similar between sham and OVX under all experimental conditions. (For basal conditions, $n = 15$ sham, 25 OVX cells from 7 sham, 12 OVX mice. For H-89, $n = 11$ sham, 17 OVX cells from 5 sham, 6 OVX mice. For 8-Br-cAMP, $n = 6$ sham, 7 OVX cells from 5 sham, 5 OVX mice. * denotes $P < 0.05$ in comparison to sham by 2-way ANOVA; † denotes $P < 0.05$ in comparison to same-group basal; dotted lines represent basal values).

between the two groups under basal conditions (Fig. 4C). This indicates that Ca^{2+} transients and caffeine transients increased in parallel in OVX myocytes. To determine whether OVX modified SR Ca^{2+} content via the cAMP/PKA pathway, caffeine transients were also measured in the presence of 2 μM H-89. SR Ca^{2+} stores were reduced by H-89 in OVX, but not sham cells, and the basal difference was eliminated (Fig. 4B). Similarly, SR Ca^{2+} content was no longer different between sham and OVX when cells were dialysed with the same concentration of 8-Br-cAMP (Fig. 4B). Fractional release also was similar in sham and OVX when cells were exposed to H-89 or 8-Br-cAMP (Fig. 4C). These results indicate that elevated SR Ca^{2+} content contributes to larger Ca^{2+} transients in OVX cells. This difference is regulated by the cAMP/PKA pathway, as differences between groups were abolished by PKA inhibition or when cAMP levels were clamped to the same concentration in sham and OVX cells.

3.4. OVX myocytes exhibit increased production and breakdown of cAMP and increased AC5 expression

We investigated whether basal differences in SR Ca^{2+} release between sham and OVX myocytes were due to higher levels of cAMP in OVX myocytes. Interestingly, Fig. 5A shows no difference in basal cAMP levels in unstimulated ventricular myocytes from sham and OVX mice. To determine whether the production of cAMP was increased in OVX in comparison to sham, cAMP levels were measured in the presence of the AC activator forskolin. Activation of AC (1 μM forskolin) increased intracellular cAMP in OVX myocytes only and resulted in higher levels than in sham cells (Fig. 5A). This difference was even greater with 10 μM forskolin. To determine if AC activity was increased following OVX, cAMP levels were measured in the presence of the non-selective PDE inhibitor IBMX (300 μM). While IBMX had no effect on intracellular cAMP levels in sham myocytes, it caused a significant increase in cAMP in OVX cells (Fig. 5A). These results demonstrate that myocytes from OVX hearts had a greater response to direct AC activation, and higher cAMP production when all PDE isoforms were inhibited, in comparison to sham controls. To determine whether increased cAMP production in OVX cells was due to increased AC expression, we performed quantitative PCR experiments to compare the expression of various cardiac AC isoforms in ventricles from sham and OVX mice. Results showed that OVX increased the mRNA expression of AC5 in the ventricles when compared to sham controls, while AC4, AC6 and AC9 isoforms were unaffected (Fig. 5B). These data demonstrate that AC5 expression is increased by OVX. Increased AC activity following withdrawal of ovarian hormones could contribute to larger contractions and Ca^{2+} transients.

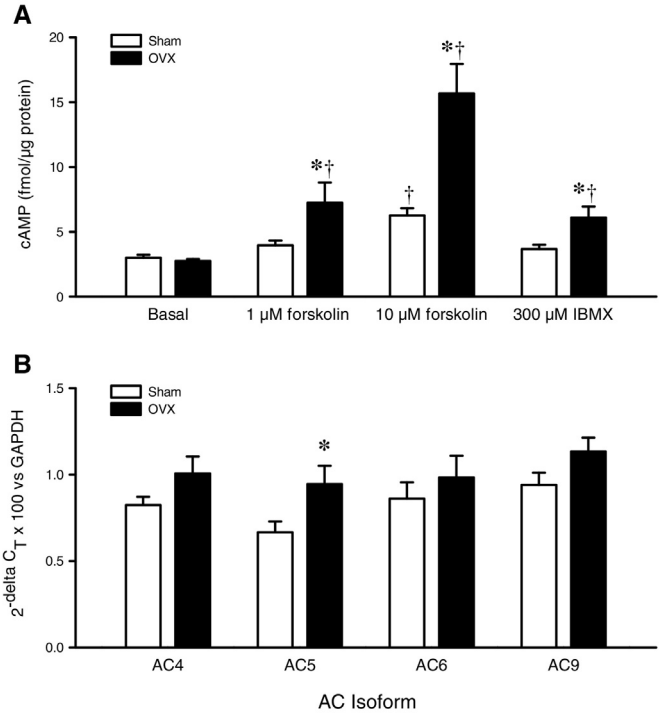

Fig. 5. Intracellular cAMP does not differ between sham and OVX in control conditions, but OVX may have increased production of cAMP by AC. A. In unstimulated ventricular myocytes, cAMP levels were similar between sham and OVX. Upon activation of AC with forskolin (1 and 10 μM), cAMP levels increased more in OVX than in sham cells. Intracellular cAMP also became higher in OVX in the presence of the non-selective PDE inhibitor IBMX. ($n = 3$ sham, 3 OVX hearts in triplicate). B. Quantitative mRNA expression of AC4, AC6, and AC9 relative to GAPDH was similar in ventricles from sham and OVX female mice, while OVX ventricles had higher levels of AC5 than sham. ($n = 5$ sham, 5 OVX hearts. * denotes $P < 0.05$ in comparison to sham by 2-way ANOVA; † denotes $P < 0.05$ in comparison to same-group basal).

3.5. PDE4A expression is increased in OVX, but rolipram only affects Ca^{2+} current in OVX myocytes

To determine if the breakdown of cAMP was affected by OVX, quantitative PCR experiments were performed to examine the expression of various cardiac PDE isoforms. Interestingly, mRNA expression of PDE4A was increased in OVX ventricles in comparison to sham, while expression of PDE 3A, 3B, 4B and 4D did not differ (Fig. 6). To investigate the impact of this difference in PDE4A expression on EC coupling mechanisms, voltage-clamp experiments were performed in the presence of the selective PDE4 inhibitor rolipram (10 μM). Ca^{2+} transients, Ca^{2+} currents and contractions were measured simultaneously in sham and OVX myocytes during a test step to 0 mV in the presence of rolipram as shown in the examples in Fig. 7A. Fig. 7B shows that rolipram had no effect on contractions in either sham or OVX myocytes (the dotted lines indicate basal values) and contractions remained larger in OVX cells than sham. Similarly, rolipram had no effect on peak Ca^{2+} transients in either group, and Ca^{2+} transients remained larger in OVX cells (Fig. 7C). Rolipram did increase Ca^{2+} current in OVX cells, so that Ca^{2+} currents were significantly larger in OVX than in sham controls (Fig. 7D). Importantly, rolipram abolished the increase in EC-coupling gain seen under basal conditions in OVX cells (Fig. 7E), likely because rolipram increased Ca^{2+} current in OVX but not sham cells. Interestingly, PDE4 inhibition also abolished the difference in SR Ca^{2+} content caused by OVX (Fig. 7F). Rolipram had no effect on diastolic Ca^{2+} levels (Fig. 7G). These results demonstrate that withdrawal of ovarian hormones increases expression of PDE4A, which may contribute to alterations in the gain of EC coupling.

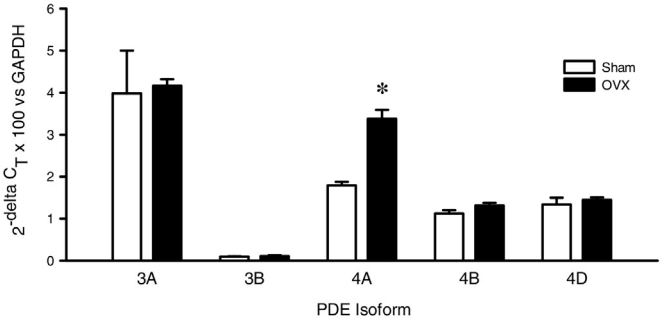

Fig. 6. Ventricles from OVX mice have higher PDE4A expression levels. Quantitative mRNA expression of PDE3A, PDE3B, PDE4B and PDE4D relative to GAPDH was similar in ventricles from sham and OVX female mice. OVX ventricles showed higher levels of PDE4A mRNA in comparison to sham. ($n = 3$ sham, 3 OVX hearts in triplicate. * denotes $P < 0.05$ in comparison to sham by 2-way ANOVA).

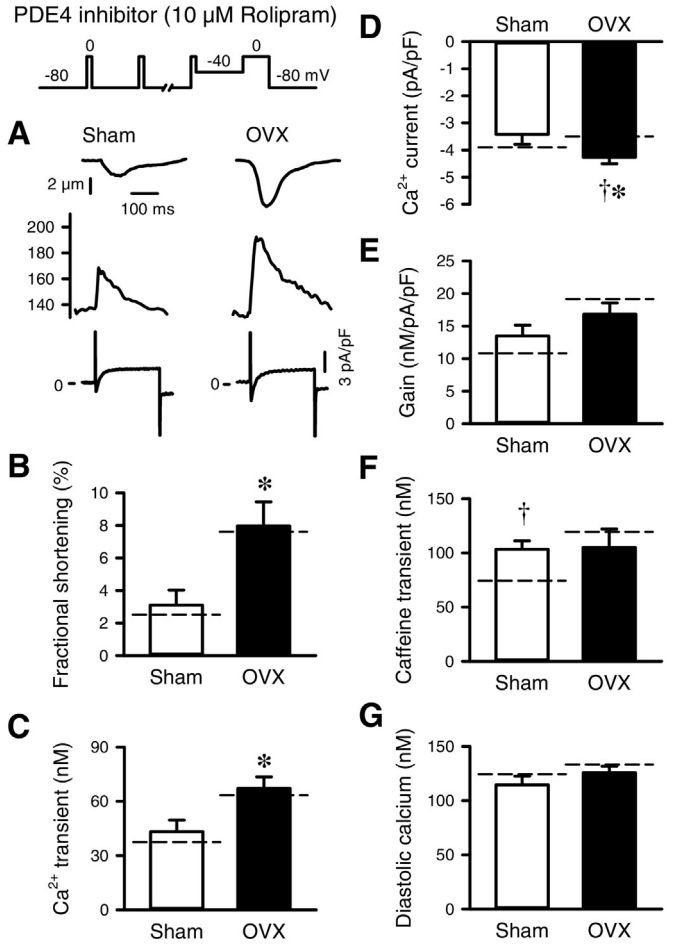

Fig. 7. Inhibition of PDE4 in sham and OVX myocytes does not affect contraction, Ca^{2+} transient or EC coupling gain, but increases Ca^{2+} current in OVX cells only. The voltage clamp protocol used is depicted in the top panel. A. Representative contractions (top), Ca^{2+} transients (middle) and Ca^{2+} currents (bottom) obtained from a sham and an OVX myocyte in the presence of the selective PDE4 inhibitor rolipram (10 μM). B. Inhibition of PDE4 did not affect contractions in sham or OVX myocytes. C. Similarly, Ca^{2+} transients were unchanged in the presence of rolipram. D. PDE4 inhibition increased Ca^{2+} current in OVX cells only, resulting in larger current in comparison to sham myocytes. E. EC coupling gain in sham and OVX was unaffected by rolipram. F. SR Ca^{2+} stores are no longer different between sham and OVX in the presence of rolipram. G. Diastolic Ca^{2+} levels were similar in sham and OVX cells in the absence or presence of rolipram. (For contractions, $n = 7$ sham, 15 OVX cells. For other parameters, $n = 12$ sham, 23 OVX cells; 8 sham, 7 OVX mice. * denotes $P < 0.05$ in comparison to sham by 2-way ANOVA; † denotes $P < 0.05$ in comparison to same-group basal; dotted lines represent basal values).

4. Discussion

This study aimed to determine whether female sex steroid hormones modify EC-coupling mechanisms via the cAMP/PKA pathway. Results show that under basal conditions, removal of ovarian hormones by OVX caused larger contractions and Ca^{2+} transients in isolated ventricular myocytes in comparison to sham-operated controls, although Ca^{2+} current was unchanged. In addition, EC-coupling gain and SR Ca^{2+} stores were higher in OVX myocytes. To investigate contributions of the cAMP/PKA pathway to these differences in EC-coupling mechanisms, either a PKA inhibitor was used or sham and OVX cells were exposed to the same concentration of intracellular cAMP. In both experimental settings, differences in contractions, Ca^{2+} transients, gain and SR Ca^{2+} stores were abolished. While intracellular cAMP did not differ in unstimulated sham and OVX ventricular myocytes, OVX myocytes responded to either AC activation or PDE inhibition with a greater increase in cAMP. The expression of both AC5 and PDE4A were higher in OVX ventricles than sham, while other isoforms were present at similar levels. When PDE4 was selectively inhibited, contractions and Ca^{2+} transients remained larger in OVX myocytes, and in fact, Ca^{2+} current became larger in comparison to sham controls. The increase in gain and SR Ca^{2+} content was eliminated with inhibition of PDE4. Overall, these findings suggest that removal of ovarian hormones disrupts SR Ca^{2+} release, in part through dysregulation of cAMP/PKA-dependent mechanisms. This could be linked to both increased production of cAMP as well as enhanced breakdown following removal of ovarian hormones.

This is the first study to simultaneously measure and characterize various EC coupling components in an OVX animal model; recordings of Ca^{2+} transient, Ca^{2+} current and contraction were made in isolated cardiomyocytes. We show for the first time that both contractions and Ca^{2+} transients were increased by almost 2-fold in OVX than sham myocytes, even though L-type Ca^{2+} current was not different. Further, we have concluded that the increase in EC coupling gain following OVX results in a dramatic increase in cardiac contraction. Previous studies have investigated some of these components of Ca^{2+} handling individually and provided evidence for larger Ca^{2+} transients and higher SR Ca^{2+} stores in OVX cells, with no difference in L-type Ca^{2+} current [10,12,25,30]. This may differ between species however, as Ca^{2+} current is increased following OVX in the rat model [23]. Still, whether these changes in Ca^{2+} homeostasis affect cardiac contractile function in OVX cells has remained controversial [7,10,40,50]. The results of the present study clearly demonstrate that there is a marked increase in myocyte contraction along with an increase in SR Ca^{2+} handling and EC-coupling gain in female mice following removal of ovarian hormones.

Little is known about mechanisms involved in Ca^{2+} dysregulation in OVX, although there is evidence that OVX enhances Ca^{2+} flux across RyR in purified SR vesicles and that this is reversed by PKA inhibition [25]. A key finding from our study is that PKA inhibition abolished differences in EC-coupling mechanisms that occur as a result of ovarian hormone withdrawal. Specifically, inhibition of PKA with H-89 abolished differences in SR Ca^{2+} release between sham and OVX by greatly decreasing peak Ca^{2+} transients in OVX myocytes. The present study further identified a role for PKA in maintaining basal EC-coupling gain and contraction in OVX myocytes. In the presence of H-89, these parameters were no longer larger in OVX than sham myocytes. PKA inhibition reduced gain in OVX cells only, which could be partially due to effects on SR Ca^{2+} stores. We identified a novel role for PKA in maintaining basal SR Ca^{2+} content in OVX myocytes, which we have previously reported is not observed in female myocytes [35]. These observations suggest that phosphorylation of key EC-coupling targets by PKA contributes to larger Ca^{2+} transients, gain and contractions in female myocytes following OVX. Previous studies have shown an increase in PKA expression and activity in OVX, which is reversed with estrogen treatment [23,25]. Together with the results of the present study, these data suggest that estrogen may suppress the cAMP/PKA pathway and thereby reduce SR Ca^{2+} release and attenuate EC-coupling gain.

Our results also show that dialysis of sham and OVX myocytes with the same concentration of 8-Br-cAMP abolished differences in EC-coupling between the two groups. Since the PDE-resistant 8-Br-cAMP analog was used, potential differences in the breakdown of cAMP by PDE between treatment groups were eliminated and phosphorylation of EC-coupling targets by PKA would be expected to be similar. Our results also found that 8-Br-cAMP abrogated the increase in SR Ca^{2+} stores caused by OVX. Under our experimental conditions, we found no significant effect of additional cAMP on SR Ca^{2+} content under basal conditions. Interestingly, previous studies have reported similar results in paced cells following β-adrenergic stimulation [43,46], although an increase in SR content has also been observed [21,32] so this is controversial. Together our findings suggest that activating PKA to a similar extent in sham and OVX myocytes abolishes differences in SR Ca^{2+} release and contractile function that occur following ovarian hormone withdrawal.

Our study found similar basal levels of intracellular cAMP in myocytes from sham and OVX mice, consistent with earlier observations in an OVX rat model [23]. This finding was somewhat unexpected, given that inhibition of PKA abolished differences in EC-coupling induced by OVX. A likely possibility is that removal of ovarian hormones does not affect total cellular cAMP levels, but instead alters the compartmentalization of specific cAMP pools. We found that stimulation of AC with forskolin (1–10 μM) caused a marked increase in cAMP production, which was much greater in OVX than sham myocytes. However, Kam et al. [23] reported no difference in cAMP levels when AC was stimulated with forskolin (0.1–100 μM) in ventricular myocytes from sham and OVX rats. These differences in results may reflect the use of rats versus mice or other experimental differences between our study and the earlier work in rats [23]; additional studies would be of interest. Further, we showed that cAMP levels were higher in OVX cells after treatment with the non-selective PDE inhibitor IBMX (300 μM). Thus, when cAMP cannot be broken down, levels are higher in OVX myocytes, which suggests that cAMP synthesis may be elevated by OVX. Consistent with this, we showed that OVX caused a marked increase in the expression of AC5 in the ventricles. As AC5 and AC6 are the two major AC isoforms present in cardiomyocytes [8,18], an increase in AC5 expression could account for higher levels of cAMP in OVX cells. This may also result in increased cAMP levels in AC5-specific compartments, as AC5 has been previously reported to localize within t-tubules, whereas AC6 resides outside the t-tubules [47]. Further work is needed to examine cAMP compartmentalization regulated by AC isoforms, and how this may be altered by sex steroid hormones. The AC5 gene is predicted to have two estrogen response elements, and AC6 is predicted to have one [41]. Whether these response elements are accessible to transcription factors and alter transcription of AC genes in response to estrogen is of interest for future studies. Together, our findings suggest that cAMP production by AC5 may be increased by ovarian hormone withdrawal and further, that ovarian hormones may attenuate the production of cAMP by lowering mRNA expression of AC5. This may be a protective effect of female sex hormones, as disruption of AC5 is protective against cardiac stress in cardiomyocytes [34].

A novel finding from our study is that removal of ovarian hormones in female mice results in an increase in the expression of cardiac PDE4A. This would be expected to increase the breakdown of cAMP in OVX ventricles in comparison to sham. Previous studies in male rodents have identified critical roles for unique PDE isoforms in regulating functional compartments of cAMP within ventricular myocytes [1,2]. For example, studies in males have found that PDE4B localizes to L-type Ca^{2+} channels [26] while both PDE3A and PDE4D have been shown to compartmentalize with RyR2 and SERCA2a [1–3,24]. However, PDE4A, among other cardiac isoforms, has not yet been shown to localize to any specific component of EC-coupling in male myocytes. Whether the localization of PDE isoforms previously reported in male cells also applies to females is not known. In fact, we have found sex differences in PDE4B expression, where its expression is higher in ventricles from female mice in comparison to males [36]. Although the PDE4A gene does not have an estrogen response element in its promoter, there are several cAMP response element-binding protein sites [41]. Therefore, changes in cAMP production in the OVX heart, such as those reported in the present study, could increase PDE4A expression via the cAMP response element-binding protein [42].

Our present results demonstrate that PDE4 inhibition with rolipram had no effect on contractions or Ca^{2+} transients in sham or OVX myocytes. On the other hand, inhibition of PDE4 increased Ca^{2+} current in OVX myocytes only, which resulted in larger Ca^{2+} currents in comparison to sham. To our knowledge, this is the first report of an increase in Ca^{2+} current upon inhibition of PDE4, without co-inhibition of other PDE isoforms. Others have reported no effect of PDE4 inhibition on Ca^{2+} current, although the sex of the animals used in this study was not specified [22]. Nonetheless, this increase in Ca^{2+} current could be exclusive to OVX models and could involve a change in compartmentalization of cAMP. In addition, OVX also increases AC5, which would be expected to increase cAMP production and could increase peak Ca^{2+} current even in the presence of higher levels of PDE4. One report suggests that the effect of AC5 on Ca^{2+} current is masked by PDE under basal conditions [47]; our results suggest that PDE4 inhibition has a greater effect following OVX, possibly due to an increase in the expression of AC5. Our findings suggest that the increase in PDE4A expression in OVX hearts is localized to L-type Ca^{2+} channels, as depicted in Fig. 8. This would promote the breakdown of cAMP in a compartment near L-type Ca^{2+} channels in OVX myocytes and thereby attenuate PKA-dependent phosphorylation of Ca^{2+} channels. It is possible that this is a protective adaptation to reduce cAMP/PKA-stimulated Ca^{2+} entry. PDE4 inhibition increases SR Ca^{2+} content in sham cells, potentially by increasing cAMP levels and increasing SR Ca^{2+} uptake by SERCA. By contrast, PDE4 inhibition has no effect on SR content in OVX cells. This suggests that PDE4 may no longer be involved in the regulation of SERCA activity following ovarian hormone removal. Additional studies are necessary to determine the localization of PDE4A and other PDE isoforms in female myocytes and to evaluate the effects on EC-coupling mechanisms. It would also be of interest to explore whether removal of ovarian hormones affects compartmentalization of cAMP.

There are some limitations to the work presented in this study. One potential limitation to our study is that total cellular cAMP levels were measured in unstimulated myocytes while the functional studies (e.g. voltage-clamp experiments) examined paced myocytes. The measurement of total cAMP within cardiomyocytes does not consider differences that may exist in subcellular localization of cAMP pools, which is especially important as we have identified sex hormone-mediated differences in the expression of PDE and AC isoforms. It is also possible that cAMP levels observed in these unstimulated myocytes are not identical to those in cells being paced. In fact, Na^{+} entry that occurs upon depolarization of myocytes has been shown to trigger cAMP production [8,9], which is consistent with this idea. In addition, OVX hearts have

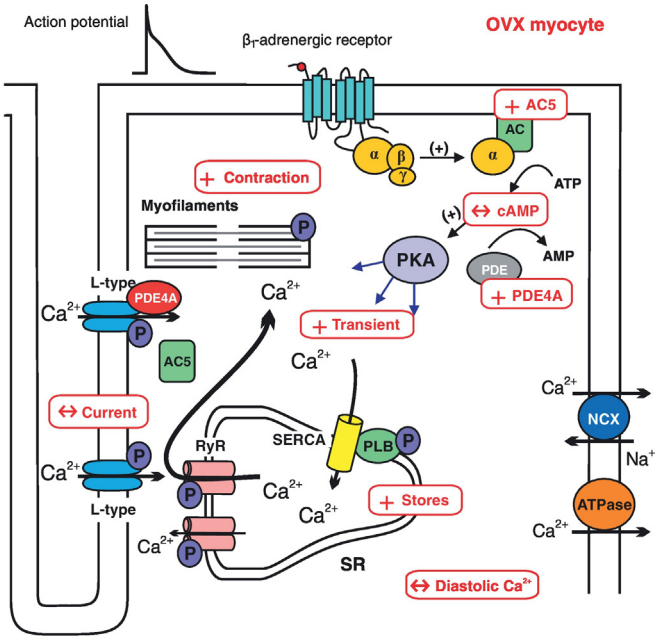

Fig. 8. Summary of effects of ovarian hormone withdrawal on EC coupling and contributions of the cAMP/PKA pathway, shown in an OVX ventricular myocyte relative to a sham-operated female control. OVX caused larger contractions and Ca^{2+} transients, which was not due to a difference in Ca^{2+} current. Diastolic Ca^{2+} was unchanged, but SR Ca^{2+} stores were higher in OVX than sham, which could contribute to increased SR Ca^{2+} release. Although unstimulated cAMP levels were similar between OVX and sham, the production of cAMP by AC and the breakdown by PDE were enhanced following OVX. These results strongly suggest alterations in the cAMP/PKA pathway contribute to the increase in contractile function and SR Ca^{2+} release in OVX myocytes, and that increased PDE4A in OVX may be localized to L-type Ca^{2+} channels.

higher NCX activity, which may remove more Ca^{2+} from the cytosol than in sham [25]. This could, in turn, enhance Na^{+} entry in OVX cells and further increase AC activation in comparison to sham. Future studies should examine cAMP levels in paced cells from sham and OVX animals. An additional possible limitation is that sources of estrogen and other sex steroid hormones other than the ovaries were not considered. While the ovaries are the major source of estrogen, tissues including adipose tissue, vascular tissue and bone express aromatase, an enzyme that can convert testosterone to 17ß-estradiol [45]. In addition, as aromatase is expressed in various tissues including the adult rodent heart, it is possible that androgens could be converted to estrogens locally, in the myocardium [4]. It is also possible that cAMP may activate pathways other than the PKA pathway to affect EC-coupling mechanisms. For example, ePAC (exchange protein directly activated by cAMP) or NOS (nitric oxide synthase) [37] are known to be activated by cAMP and may also differ between OVX and sham cardiomyocytes. Finally, we investigated PDE and AC isoforms as well as cAMP production in sham and OVX females, but have not done a male-female comparison. These are important areas for further investigation.

Clinical observations have identified an increase in the risk of cardiovascular disease in post-menopausal women [6,14,16], which could be due to the loss of ovarian hormones. We have clearly shown that ovarian hormone withdrawal directly affects intracellular Ca^{2+} regulation and cardiac contractile function. We have also shown that this is mediated, at least in part, by effects on SR Ca^{2+} release that are modulated by the cAMP/PKA pathway following ovarian hormone withdrawal. Our results highlight a critical role for estrogen in attenuating SR Ca^{2+} release and reducing the gain of EC-coupling and suggest that this effect of estrogen may be mediated by the cAMP/PKA pathway. Our results specifically indicate that estrogen may inhibit both the production and breakdown of cAMP. Compartmentalization of these effects via localization of PDE isoforms could have selective effects on Ca^{2+} currents and/or Ca^{2+} transients. Changes in the production and breakdown of cardiac cAMP following the loss of ovarian hormones could heighten responses to stimulation of the cAMP/PKA pathway via the sympathetic nervous system, which could increase SR Ca^{2+} release in situations of higher cardiac demand. Elevated SR Ca^{2+} release and higher SR Ca^{2+} content would increase the risk for Ca^{2+} overload in cardiomyocytes, which is known to contribute to cardiovascular disease [48]. Indeed, the loss of ovarian hormones may increase the risk of developing diseases such as Takotsubo cardiomyopathy and arrhythmias in older women [38,39] by enhancing cAMP/PKA-dependent SR Ca^{2+} release. Overall, this study contributes important translational knowledge towards understanding how ovarian hormones regulate specific subcellular cardiomyocyte mechanisms, and how changes in hormone levels may promote pathological conditions in older women.

Supplementary data to this article can be found online at http://dx.doi.org/10.1016/j.yjmcc.2017.07.118.

Acknowledgements

The authors express their appreciation for excellent technical assistance provided by Dr. Jie-quan Zhu and Peter Nicholl.

Funding sources

This study was supported by grants from the Canadian Institutes for Health Research [grant number MOP 97973 to SEH]. Randi Parks was supported by studentship awards from the Nova Scotia Health Research Foundation and the Dalhousie Medical Research Foundation.

Disclosures

None declared.

References

[1] S. Beca, R. Aschars-Sobbi, B.K. Panama, P.H. Backx, Regulation of murine cardiac function by phosphodiesterases type 3 and 4, Curr. Opin. Pharmacol. 11 (6) (2011) 714–719.
[2] S. Beca, P.B. Helli, J.A. Simpson, D. Zhao, G.P. Farman, P.P. Jones, X. Tian, L.S. Wilson, F. Ahmad, S.R. Chen, M.A. Movsesian, V. Manganiello, D.H. Maurice, M. Conti, P.H. Backx, Phosphodiesterase 4D regulates baseline sarcoplasmic reticulum Ca2+ release and cardiac contractility, independently of L-type Ca2+ current, Circ. Res. 109 (9) (2011) 1024–1030.
[3] S. Beca, F. Ahmad, W. Shen, J. Liu, S. Makary, N. Polidovitch, J. Sun, S. Hockman, Y.W. Chung, M. Movsesian, E. Murphy, V. Manganiello, P.H. Backx, Phosphodiesterase type 3A regulates basal myocardial contractility through interacting with sarcoplasmic reticulum calcium ATPase type 2a signaling complexes in mouse heart, Circ. Res. 112 (2) (2013) 289–297.
[4] J.R. Bell, K.M. Mellor, A.C. Wollermann, W.T. Ip, M.E. Reichelt, S.J. Meachem, E.R. Simpson, L.M. Delbridge, Aromatase deficiency confers paradoxical postischemic cardioprotection, Endocrinology 152 (12) (2011) 4937–4947.
[5] D.M. Bers, Calcium cycling and signaling in cardiac myocytes, Annu. Rev. Physiol. 70 (2008) 23–49.
[6] P. Bhupathy, C.D. Haines, L.A. Leinwand, Influence of sex hormones and phytoestrogens on heart disease in men and women, Women's Health (Lond. Engl.) 6 (1) (2010) 77–95.
[7] T. Bupha-Intr, J. Wattanapermpool, J.R. Pena, B.M. Wolska, R.J. Solaro, Myofilament response to Ca2+ and Na+/H+ exchanger activity in sex hormone-related protection of cardiac myocytes from deactivation in hypercapnic acidosis, Am. J. Physiol. Regul. Integr. Comp. Physiol. 292 (2) (2007) R837–43.
[8] D.M. Cooper, Regulation and organization of adenylyl cyclases and cAMP, Biochem. J. 375 (Pt 3) (2003) 517–529.
[9] D.M. Cooper, M.J. Schell, P. Thorn, R.F. Irvine, Regulation of adenylyl cyclase by membrane potential, J. Biol. Chem. 273 (42) (1998) 27703–27707.
[10] C.L. Curl, I.R. Wendt, B.J. Canny, G. Kotsanas, Effects of ovariectomy and 17 beta-oestradiol replacement on [Ca2+]i in female rat cardiac myocytes, Clin. Exp. Pharmacol. Physiol. 30 (7) (2003) 489–494.
[11] M.P. Czubryt, L. Espira, L. Lamoureux, B. Abrenica, The role of sex in cardiac function and disease, Can. J. Physiol. Pharmacol. 84 (1) (2006) 93–109.
[12] E. Fares, R.J. Parks, J.K. Macdonald, J.M. Egar, S.E. Howlett, Ovariectomy enhances SR Ca(2)(+) release and increases Ca(2)(+) spark amplitudes in isolated ventricular myocytes, J. Mol. Cell. Cardiol. 52 (1) (2012) 32–42.
[13] G. Grynkiewicz, M. Poenie, R.Y. Tsien, A new generation of Ca2+ indicators with greatly improved fluorescence properties, J. Biol. Chem. 260 (6) (1985) 3440–3450.
[14] S.M. Harman, Estrogen replacement in menopausal women: recent and current prospective studies, the WHI and the KEEPS, Gend. Med. 3 (4) (2006) 254–269.
[15] S.M. Harman, D.M. Black, F. Naftolin, E.A. Brinton, M.J. Budoff, M.I. Cedars, P.N. Hopkins, R.A. Lobo, J.E. Manson, G.R. Merriam, V.M. Miller, G. Neal-Perry, N. Santoro, H.S. Taylor, E. Vittinghoff, M. Yan, H.N. Hodis, Arterial imaging outcomes and cardiovascular risk factors in recently menopausal women: a randomized trial, Ann. Intern. Med. 161 (4) (2014) 249–260.
[16] C.S. Hayward, R.P. Kelly, P. Collins, The roles of gender, the menopause and hormone replacement on cardiovascular function, Cardiovasc. Res. 46 (1) (2000) 28–49.
[17] H.N. Hodis, W.J. Mack, R. Lobo, Postmenopausal hormone replacement therapy as antiatherosclerotic therapy, Curr. Atheroscler. Rep. 4 (1) (2002) 52–58.
[18] B. Hope, Laughter keeps Bob Hope young. Interview by Willah Weddon, Mich. Med. 79 (35) (1980) 650.
[19] R. Hua, A. Adamczyk, C. Robbins, G. Ray, R.A. Rose, Distinct patterns of constitutive phosphodiesterase activity in mouse sinoatrial node and atrial myocardium, PLoS One 7 (10) (2012) e47652.
[20] S. Hulley, D. Grady, T. Bush, C. Furberg, D. Herrington, B. Riggs, E. Vittinghoff, Randomized trial of estrogen plus progestin for secondary prevention of coronary heart disease in postmenopausal women. Heart and Estrogen/progestin Replacement Study (HERS) Research Group, JAMA 280 (7) (1998) 605–613.
[21] M. Hussain, C.H. Orchard, Sarcoplasmic reticulum Ca2+ content, L-type Ca2+ current and the Ca2+ transient in rat myocytes during beta-adrenergic stimulation, J. Physiol. 505 (Pt 2) (1997) 385–402.
[22] K. Kajimoto, N. Hagiwara, H. Kasanuki, S. Hosoda, Contribution of phosphodiesterase isozymes to the regulation of the L-type calcium current in human cardiac myocytes, Br. J. Pharmacol. 121 (8) (1997) 1549–1556.
[23] K.W. Kam, G.M. Kravtsov, J. Liu, T.M. Wong, Increased PKA activity and its influence on isoprenaline-stimulated L-type Ca2+ channels in the heart from ovariectomized rats, Br. J. Pharmacol. 144 (7) (2005) 972–981.
[24] B.G. Kerfant, D. Zhao, I. Lorenzen-Schmidt, L.S. Wilson, S. Cai, S.R. Chen, D.H. Maurice, P.H. Backx, PI3Kgamma is required for PDE4, not PDE3, activity in subcellular microdomains containing the sarcoplasmic reticular calcium ATPase in cardiomyocytes, Circ. Res. 101 (4) (2007) 400–408.
[25] G.M. Kravtsov, K.W. Kam, J. Liu, S. Wu, T.M. Wong, Altered Ca(2+) handling by ryanodine receptor and Na(+)-Ca(2+) exchange in the heart from ovariectomized rats: role of protein kinase A, Am. J. Physiol. Cell Physiol. 292 (5) (2007) C1625–35.
[26] J. Leroy, W. Richter, D. Mika, L.R. Castro, A. Abi-Gerges, M. Xie, C. Scheitrum, F. Lefebvre, J. Schittl, P. Mateo, R. Westenbroek, W.A. Catterall, F. Charpentier, M. Conti, R. Fischmeister, G. Vandecasteele, Phosphodiesterase 4B in the cardiac L-type Ca(2)(+) channel complex regulates Ca(2)(+) current and protects against ventricular arrhythmias in mice, J. Clin. Invest. 121 (7) (2011) 2651–2661.
[27] R.A. Lobo, The hope for KEEPS, Climacteric 18 (2) (2015) 108–109.
[28] E.D. Luczak, L.A. Leinwand, Sex-based cardiac physiology, Annu. Rev. Physiol. 71 (2009) 1–18.

[29] T. Luo, J.K. Kim, The role of estrogen and estrogen receptors on cardiomyocytes: an overview, Can. J. Cardiol. 32 (8) (2016) 1017–1025.
[30] Y. Ma, W.T. Cheng, S. Wu, T.M. Wong, Oestrogen confers cardioprotection by suppressing Ca2 +/calmodulin-dependent protein kinase II, Br. J. Pharmacol. 157 (5) (2009) 705–715.
[31] J.E. Manson, J. Hsia, K.C. Johnson, J.E. Rossouw, A.R. Assaf, N.L. Lasser, M. Trevisan, H.R. Black, S.R. Heckbert, R. Detrano, O.L. Strickland, N.D. Wong, J.R. Crouse, E. Stein, M. Cushman, Estrogen plus progestin and the risk of coronary heart disease, N. Engl. J. Med. 349 (6) (2003) 523–534.
[32] J.T. Maxwell, T.L. Domeier, L.A. Blatter, beta-Adrenergic stimulation increases the intra-SR Ca termination threshold for spontaneous Ca waves in cardiac myocytes, Channels (Austin) 7 (3) (2013) 206–210.
[33] V.M. Miller, D.M. Black, E.A. Brinton, M.J. Budoff, M.I. Cedars, H.N. Hodis, R.A. Lobo, J.E. Manson, G.R. Merriam, F. Naftolin, N. Santoro, H.S. Taylor, S.M. Harman, Using basic science to design a clinical trial: baseline characteristics of women enrolled in the Kronos Early Estrogen Prevention Study (KEEPS), J. Cardiovasc. Transl. Res. 2 (3) (2009) 228–239.
[34] S. Okumura, J. Kawabe, A. Yatani, G. Takagi, M.C. Lee, C. Hong, J. Liu, I. Takagi, J. Sadoshima, D.E. Vatner, S.F. Vatner, Y. Ishikawa, Type 5 adenylyl cyclase disruption alters not only sympathetic but also parasympathetic and calcium-mediated cardiac regulation, Circ. Res. 93 (4) (2003) 364–371.
[35] R.J. Parks, S.E. Howlett, H-89 decreases the gain of excitation-contraction coupling and attenuates calcium sparks in the absence of beta-adrenergic stimulation, Eur. J. Pharmacol. 691 (1–3) (2012) 163–172.
[36] R.J. Parks, G. Ray, L.A. Bienvenu, R.A. Rose, S.E. Howlett, Sex differences in SR Ca release in murine ventricular myocytes are regulated by the cAMP/PKA pathway, J. Mol. Cell Cardiol. 75 (2014) 162–173.
[37] L. Pereira, D.J. Bare, S. Galice, T.R. Shannon, D.M. Bers, beta-Adrenergic induced SR Ca2 + leak is mediated by an Epac-NOS pathway, J. Mol. Cell. Cardiol. 108 (2017) 8–16.
[38] R.W. Peters, M.R. Gold, The influence of gender on arrhythmias, Cardiol. Rev. 12 (2) (2004) 97–105.
[39] V. Regitz-Zagrosek, U. Seeland, Sex and gender differences in clinical medicine, Handb. Exp. Pharmacol. 214 (2012) 3–22.
[40] J. Ren, K.K. Hintz, Z.K. Roughead, J. Duan, P.B. Colligan, B.H. Ren, K.J. Lee, H. Zeng, Impact of estrogen replacement on ventricular myocyte contractile function and protein kinase B/Akt activation, Am. J. Physiol. Heart Circ. Physiol. 284 (5) (2003) H1800–7.
[41] SABiosciences-Qiagen, http://www.sabiosciences.com/chipqpcr.php 2012 (Retrieved August 13, 2014).
[42] W.A. Sands, T.M. Palmer, Regulating gene transcription in response to cyclic AMP elevation, Cell. Signal. 20 (3) (2008) 460–466.
[43] R. Sankaranarayanan, Y. Li, D.J. Greensmith, D.A. Eisner, L. Venetucci, Biphasic decay of the Ca transient results from increased sarcoplasmic reticulum Ca leak, J. Physiol. 594 (3) (2016) 611–623.
[44] R.H. Shutt, S.E. Howlett, Hypothermia increases the gain of excitation-contraction coupling in guinea pig ventricular myocytes, Am. J. Physiol. Cell Physiol. 295 (3) (2008) C692–700.
[45] E.R. Simpson, Sources of estrogen and their importance, J. Steroid Biochem. Mol. Biol. 86 (3–5) (2003) 225–230.
[46] L.S. Song, S.Q. Wang, R.P. Xiao, H. Spurgeon, E.G. Lakatta, H. Cheng, beta-Adrenergic stimulation synchronizes intracellular Ca(2 +) release during excitation-contraction coupling in cardiac myocytes, Circ. Res. 88 (8) (2001) 794–801.
[47] V. Timofeyev, R.E. Myers, H.J. Kim, R.L. Woltz, P. Sirish, J.P. Heiserman, N. Li, A. Singapuri, T. Tang, V. Yarov-Yarovoy, E.N. Yamoah, H.K. Hammond, N. Chiamvimonvat, Adenylyl cyclase subtype-specific compartmentalization: differential regulation of L-type Ca2 + current in ventricular myocytes, Circ. Res. 112 (12) (2013) 1567–1576.
[48] M. Vassalle, C.I. Lin, Calcium overload and cardiac function, J. Biomed. Sci. 11 (5) (2004) 542–565.
[49] G.L. Wells, Cardiovascular risk factors: does sex matter? Curr. Vasc. Pharmacol. 14 (5) (2016) 452–457.
[50] Q. Wu, Z. Zhao, H. Sun, Y.L. Hao, C.D. Yan, S.L. Gu, Oestrogen changed cardiomyocyte contraction and beta-adrenoceptor expression in rat hearts subjected to ischaemia-reperfusion, Exp. Physiol. 93 (9) (2008) 1034–1043.
[51] W. Yuan, D.M. Bers, Protein kinase inhibitor H-89 reverses forskolin stimulation of cardiac L-type calcium current, Am. J. Phys. 268 (3 Pt 1) (1995) C651–9.